Modeling the Effect of Hydration in Zeolite Na^+−Mordenite

G. Maurin,*,† R. G. Bell,† S. Devautour,‡ F. Henn,‡ and J. C. Giuntini‡

The Davy Faraday Research Laboratory, Royal Institution of Great Britain, 21 Albemarle Street, London W1S 4BS, United Kingdom. Laboratoire de Physicochimie de la Matière Condensée, Université Montpellier II, Pl. E. Bataillon, 34095 Montpellier Cedex 05, France

Received: January 20, 2003; In Final Form: January 28, 2004

A microscopic description of the effect of hydration on the behavior of extraframework cations in zeolite Na^+−mordenite is reported. Energy minimization techniques, combined with appropriate interatomic potentials to describe the potential energy surface of this complex system, have been used to determine the site selectivity of both cations and water molecules as a function of the hydration level. We have thus shown that the positions of the cations in the main channels are substantially perturbed upon the sorption of water molecules whereas those of the cations located in the small side channels are only slightly shifted. This modeling has been successfully compared with experimental data obtained by dielectric relaxation spectroscopy.

Introduction

Due to their unique characteristics, zeolites are involved in a large domain of chemical science and technology including catalytic and separation processes, storage of adsorbed molecules[3] and ion exchange.[1−4] Many research efforts performed both experimentally and theoretically, have been thus focused on this class of materials not only because of their technological importance but also because they represent model systems for a wide range of investigations, including structural properties of the framework and static or dynamic behavior of various fluids in their confined geometries.[5] The aluminosilicate framework of the zeolites is characterized by pore systems consisting of channels and cages. The anionic character of the lattice due to the substitution of silicon by aluminum is neutralized by exchangeable cations located in very well-defined surface sites surrounded by oxygen atoms of the framework.[6] A knowledge of the partition of these extraframework cations among the different sites is a crucial point because it influences the distribution of the electron density in the framework[7] and hence the interactions with the adsorbed molecules, leading to changes in the adsorption and catalytic properties of the zeolites. Here we have focused our attention on a typical zeolite Na^+−mordenite characterized by the ideal composition $Na_8Al_8Si_{40}O_{96}$, $n H_2O$ with n ranging from 0 (dehydrated state) to 24 (totally hydrated state).[8] Its structure is orthorhombic (*Cmcm*) with unit cell parameters $a = 18.1$ Å, $b = 20.5$ Å, and $c = 7.5$ Å. The framework has a porous structure which consists of main channels having a slightly elliptical cross section with 12 TO_4 tetrahedron units (T = Si, Al) and connected to small side channels via double eight-membered rings (Figure 1). The location of the cations in dehydrated Na^+ mordenite was investigated both experimentally by dielectric relaxation spectroscopy (DRS)[9,10] and theoretically by combining a pair potential model with a simulated annealing procedure.[11] We have shown that the simulated positions of the extraframework cations and their occupancies were in good agreement with the experimental data. The cations in the dehydrated Mordenite are located half in the main channels (sites IV and VI) and half in the small side channels (site I) (Figure 2).

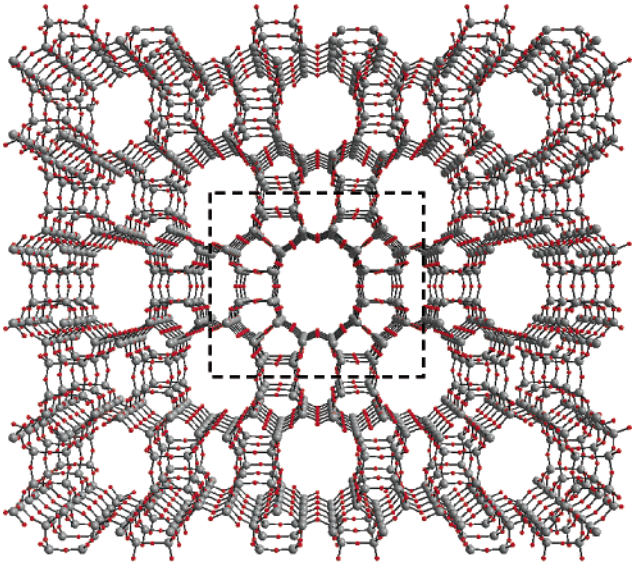

Figure 1. Representation of the mordenite framework. The unit cell is delimited by dash lines.

The next step of this work was to explore the effect of water on both the distribution of the extraframework cations and on their interactions with the framework by means of DRS.[12] From a practical point of view, this study was performed because water plays a key role in many applications involving adsorption and, more particularly, in ion exchange carried out in aqueous solution. In the latter case, it is well-known that water improves the efficiency of this process by coordinating the cations and hence increasing their mobility.[13,14] Furthermore, it was the first attempt to elucidate the distribution of the 24 H_2O among the 36 possible sites grouped in 5 different crystallographic sites named II(w), III(w), IV(w), V(w), and VI(w) (Figure 3) according to the classification established by Mortier.[6]

We showed then experimentally that the cations are progressively detrapped from their initial occupied sites in the

* To whom correspondence should be addressed. E-mail: gmaurin@ri.ac.uk. Phone: +33 4 91 63 71 17. Fax: +33 4 91 63 71 11.
† Royal Institution of Great Britain.
‡ Université Montpellier II.

10.1021/jp034151a CCC: $27.50
Published on Web 02/27/2004

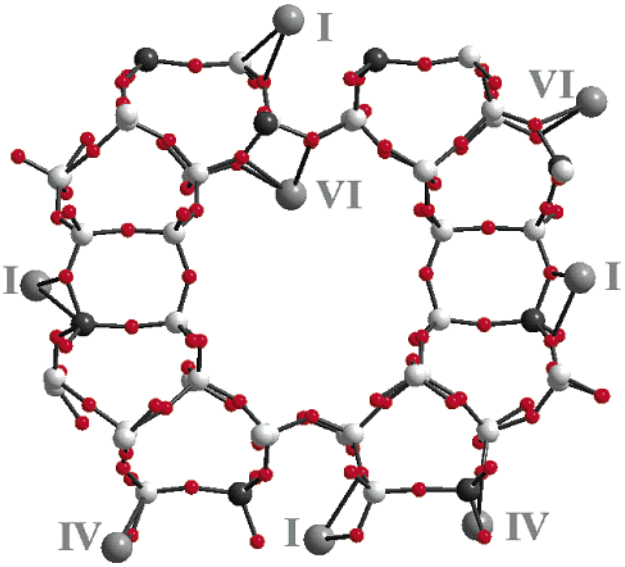

Figure 2. Typical (Si, Al) mordenite lattice used for the simulation. Distribution of the extraframework cations in the dehydrated structure among the 3 distinct crystallographic cation sites I, IV, and VI.

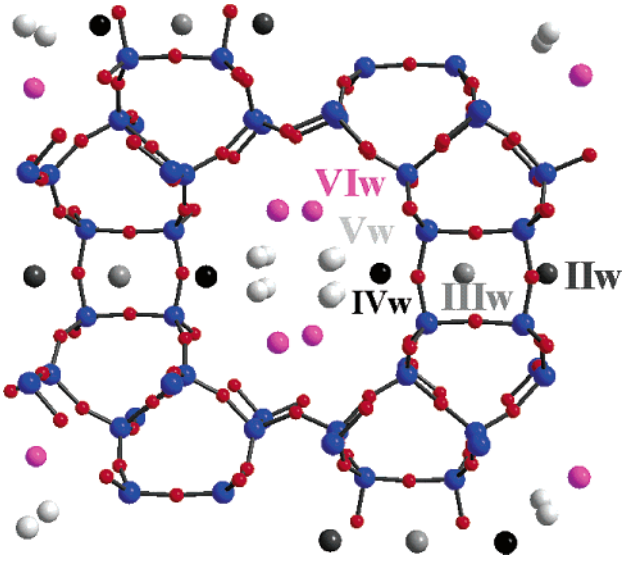

Figure 3. Unit cell of mordenite and description of the 36 crystallographic sites for water named IIw, IIIw, IVw, Vw, and VIw according to Mortier's classification.

dehydrated state, as the number of water molecules per unit cell is increased up to 24 H_2O, corresponding to the totally hydrated structure. Furthermore, we have pointed out a weakening of the interactions between the extraframework cations and the zeolite framework with increasing water content. These observations were in accordance with other experiments performed on various zeolites.[15,16]

Our aim is now to follow a similar approach to that which we successfully applied in the case of the dehydrated Na^+−mordenite,[11] to model the hydration process in this zeolite. Here, we propose to provide a microscopic description of the effect of water on the exchangeable cations behavior by means of atomistic simulation.

To study this complex system, the first step, which appears very crucial, is to select a water potential able to reproduce well the interactions involved in the whole system. To this end, some attempts have been already made to study various zeolite systems.[17−27] Among the first reported work, molecular dynamics simulations on hydrated zeolite A successfully reproduced the locations of the extraframework cations.[18,19] Later, some studies were performed on more complex zeolites, such as Na−MAP and Na−clinoptilolite, but in these cases, the authors encountered many difficulties in reproducing the experimental data.[20,23] A possible explanation of these discrepancies would be due to an inadequate potential model, which overstated the influence of hydration on the zeolite structure. Finally, the most significant work has been recently done by Lewis and Ruiz Salvador et al.[25,26] and De Leeuw et al.,[27] who reported successful modeling of the hydration on natural zeolites and on zeolite A, respectively. In both of these studies, the interatomic potentials used to describe the potential energy surface of these complex zeolite systems appeared to be very reliable and were partially selected in our model. We first present the methodology that we followed to build the structure of the fully hydrated Na^+−mordenite, and we report the simulation results that are then compared with our experimental data before giving some concluding remarks.

Computational Methodology

In a first step, we selected a typical (Si,Al) mordenite lattice, characterized by Si/Al = 5, from representative aluminum configurations previously obtained by combining solid state ^{29}Si NMR spectroscopy data and Monte Carlo simulation.[11,28] The location of the extraframework cations in the totally dehydrated state was then determined by means of the energy minimization code *GULP* (General Utility Lattice Program).[29] The starting positions for these sodium cations were chosen so as to be consistent with our previous work,[11] which showed that the extraframework cations are always located close to the aluminum atoms. We therefore introduced these cations in such a way that they were in the same channels as the aluminum atoms. The calculation was performed using periodic boundary conditions and the crystallographic unit cell of mordenite $Si_{40}Al_8O_{96}$-Na_8 with space group *P*1 to avoid any symmetry constraint. Energy minimization consisted of a combination of the Newton−Raphson method, updating the Hessian matrix by the BFGS (Broyden, Fletcher Goldfarb, and Shanno) approach and the RFO (rational function optimization) technique, which allowed us to reach a "true minimum", rejecting other stationary states.[29] The potential energy surface of the system was evaluated by an appropriate pair potential model. For this purpose, we used the potentials reported by Jackson and Catlow[30] (which includes the Sanders et al.[31]) to describe the interactions within the zeolite framework and between the framework and the extraframework cations. In this model, the zeolite framework is considered to be fully flexible by introducing a three body term for O−Al−O and O−Si−O, and polarizable via a shell model for the oxygen atoms. The intermolecular interactions between all the atoms are given by Buckingham potentials. The pair potential parameters and the charges carried by the atoms are listed in Table 1. The Ewald summation was used for the calculation of the Coulomb interactions and the short-range contribution was evaluated by introducing a cutoff at 16 Å.[32,33] The final cation equilibrium positions have been checked by the numerical evaluation of the derivatives of the potential energy surface with respect to the whole system displacement. A suitable convergence of the gradient and the Hessian positive definite confirmed that the equilibrium positions have indeed been found.

The locations of the extraframework cations thus defined for the selected (Si,Al) dehydrated mordenite lattice are reported in Figure 2. We find that four cations are split equally between sites IV and VI in the main channels and four are located on sites I in the small side channels. It is thus apparent that our

TABLE 1: Pair Potential Parameters and Charges Carried by the Atoms Used To Describe the Interactions within the Framework and between the Framework and the Extraframework Cations

species	charge/e	core−shell interactions/eV·Å^{-2}
Al	3.00000	
Si	4.00000	
Na	1.00000	
O (core)	0.86902	
O (shell)	−2.86902	74.92

Buckingham Potential (Short-Range Cutoff: 16 Å)

ion pair	*A*/eV	*ρ*/Å	*C*/eV·Å^6
Si−O	1283.907	0.32052	10.66158
Al−O	1460.300	0.29912	0.00000
Na−O	1226.840	0.30650	0.00000
O−O	22764.000	0.14900	27.88000

Three-Body Potential

	k/eV·rad^{-2}	*θ*/deg
O−Si−O	2.09724	109.47
O−Al−O	2.09724	109.47

chosen Al configuration is particularly judicious because it leads to a cation distribution close to those observed experimentally by X-ray diffraction[34] and dielectric relaxation spectroscopy.[9,10] As a statistical treatment of the effect of hydration on a sample of mordenite lattices corresponding to various distributions of the Al atoms would be very highly computationally demanding and thus unfeasible, this observation is noteworthy because it justifies the use of this configuration in developing a microscopic description of the effect of hydration on Na^+−mordenite. As previously mentioned, we also had to choose a water potential among the different ones available in the literature.[35] The potential developed by De Leeuw et al. for the modeling of polarizable water molecules was then selected.[27,36] This water potential, which includes polarizability of the oxygen atoms via the shell model appeared particularly compatible with the potential models used for the zeolite framework, and it has been successfully used for the modeling of water adsorption onto ionic mineral surfaces[36] and more recently for the simulation of hydrated zeolites.[27] The potential parameter set for water molecules, which was empirically fitted to reproduce the experimental data of both water monomer and dimer, is reported in Table 2. It consists of a Morse potential to define the O−H bond, a three-body term for H−O−H and short-range interactions described by a Lennard-Jones potential between oxygen atoms, and a Buckingham term between hydrogen and oxygen atoms. Parts of the electrostatic interactions between H−H and O−H are removed to take into account the steric effect of the electron lone pairs on the oxygen atom.

Finally, the interactions between the water molecules and the zeolite framework were taken from the work of Lewis et al.,[26] which modified the potential deduced by De Leeuw et al.[36] for the mineral surfaces, to make it suitable for zeolites. The short-range interactions between both the zeolite framework and extraframework cations, and water oxygen atoms are represented by Buckingham potentials with the parameters listed in the Table 3.

Once the potential energy surface was thus defined, we built the structure of the fully hydrated Na^+−mordenite containing 24 water molecules per unit cell. We started from the selected dehydrated aluminum configuration and inserted the water molecules step by step by adopting the following methodology. We first probed the 36 crystallographic sites previously described (Figure 3) by introducing in each of them 1 water molecule. This insertion was performed by using Accelrys Cerius^2 software,[37] which allows us to put the oxygen atoms in the sites reported by the X-ray diffraction data[8] and then to generate the hydrogen positions manually. We then minimized these 36 generated structures to select the most stable for the next adding step. We repeated this procedure for each hydration rate until we reached the structure of the fully hydrated Na^+−mordenite. However, due to the complexity of the potential energy surface, we had to adopt a stepwise minimization approach to reach a convergence to the lowest energy structures. This consisted first of minimizing only the water molecule positions under constant volume followed by an optimization of the extraframework cations and then of the zeolite framework under constant volume. Finally, a minimization of the whole structure was performed under constant pressure. This highly computationally demanding methodology was the only way that guaranteed us to reach a suitable convergence of the gradient. However, due to the unknown orientations of the water hydrogen atoms, we observed a multitude of local minima for each given hydration state. To avoid this problem, we generated, for each hydration state, several starting configurations corresponding to different orientations of the water hydrogen atoms. This complex route allowed us to isolate the lowest energy structures corresponding to hydration levels ranging from 1 to 24 water molecules per unit cell.

TABLE 2: Pair Potential Parameters and Charges for Water Molecules[a]

species	charge/e	core−shell interactions/ eV·Å^{-2}
H	0.40000	
Ow (core)	1.25000	
Ow (shell)	−2.05000	209.449602

Lennard Jones Potential (Short-Range Cutoff: 16 Å) (A/r^{12}-B/r^6)

ion pair	A/eV·Å^{12}	B/eV·Å^6
Ow−Ow	39344.98	42.15

Buckingham Potential (Short-Range Cutoff: 16 Å) ($A.\exp(-\rho r)$-C/r^6)

ion pair	*A*/eV	*ρ*/Å	*C*/eV·Å^6
H−Ow	396.270	0.25000	10.00000

Morse Potential ($D([1 - \exp(-a(r - r_o))]^2 - 1)$)

	D/eV	*a*/Å^{-1}	r_o/Å
H−Ow	6.203713	2.22003	0.92376

Three-Body Potential ($k(\theta - \theta_0)^2$)

	k/eV rad^{-2}	θ_0/deg
H−Ow−H	4.19980	108.69

Intramolecular Coulombic Subtraction (%)

H−H	50
Ow−H	50

[a] O_w represents the oxygen of the water molecules.

TABLE 3: List of Parameters To Describe Both the Interactions between the Framework and the Extraframework Cations and the Water Molecules

Buckingham Potential (Short-Range Cutoff: 16 Å)

ion pair	*A*/eV	*ρ*/Å	*C*/eV·Å^6
Si−Ow	1283.907	0.32052	10.66158
Al−Ow	1460.300	0.29912	0.00000
Na−Ow	1226.840	0.30650	0.00000
O−Ow	22764.000	0.14900	28.92000

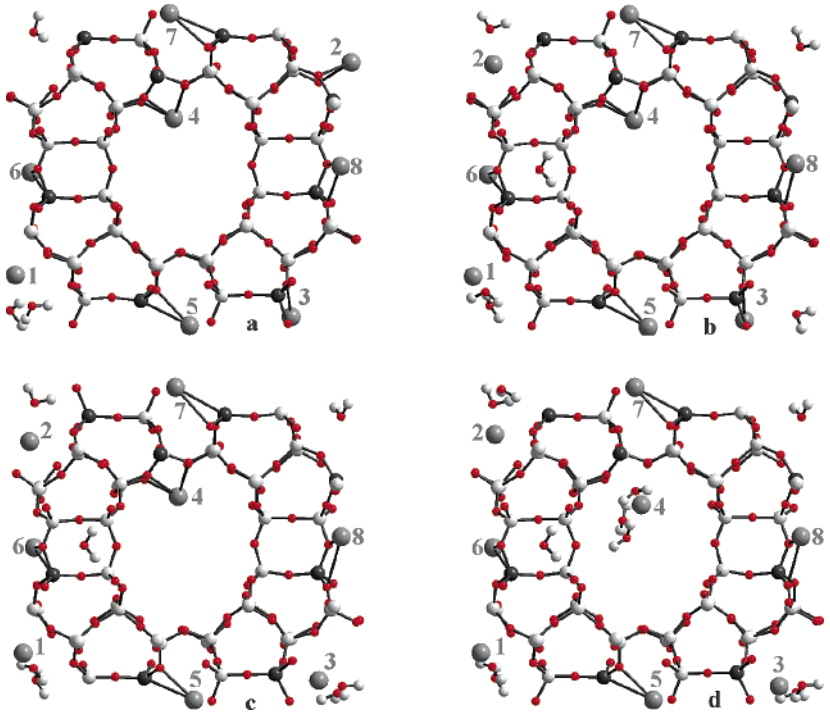

Figure 4. Evolution of the extraframework cation positions as a function of the water content: (a) 3 H_2O/uc; (b) 6 H_2O/uc; (c) 7 H_2O/uc; (d) 11 H_2O/uc.

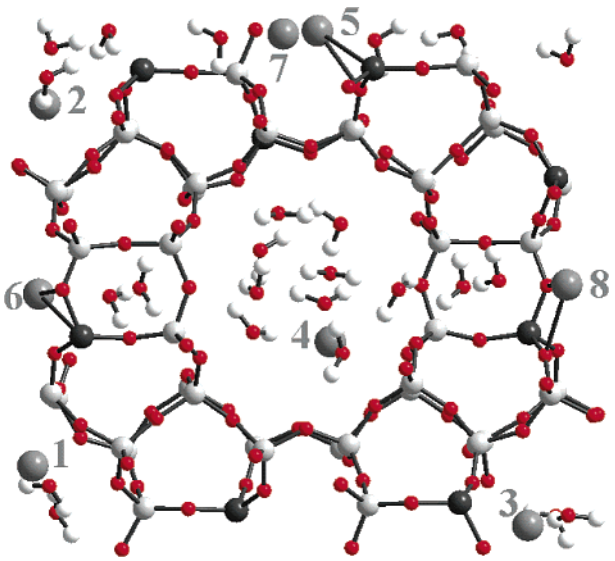

Figure 5. Representation of the fully hydrated Na^+−mordenite.

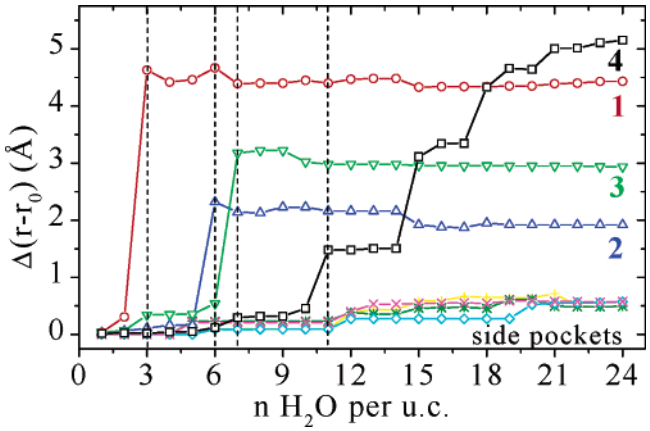

Figure 6. Evolution of the displacement for each cations from their initial positions in the dehydrated structure as a function of the number of water molecules per unit cell.

Results and Discussion

First of all, we were interested in following the cation positions as a function of the number of water molecules. We observed that the two first water molecules do not interact strongly with the cations. However, the introduction of the third leads to the detrapping of the first cation named 1, initially located in site IV (Figure 4a). In the same way, the sixth and the seventh water molecules extract cations 2 and 3 from their initial sites VI and IV, respectively, as shown in Figure 4b,c. Next, a significant motion of cation 4, situated on site VI in the main channel, occurs for eleventh water (Figure 4d). Subsequently, we note that adding the next H_2O molecules, up to twentieth, gives rise to the migration of cation 4 toward the center of the channel. Finally, the four last waters, which are located in sites IIw, cause a slight shift of the cations situated in the neighboring small side channels (sites I). We then reach the structure of the fully hydrated mordenite, presented in Figure 5. This hydration process can be also followed by evaluating the cation displacements from their initial sites as a function of the hydration level (Figure 6). We can observe that cations 1−3 are significantly shifted after adsorption of 3, 6, and 7 water molecules, respectively, and then experience only small displacements at higher hydration. By contrast, cation 4 undergoes quasi-continuous displacement from 11 water molecules upward along the hydration process, leading progressively to its final site near the center of the main channel. Finally, the cations located in the small side channels (sites I) move only slightly from their initial positions (less than 0.5 Å).

For a crystallographic point of view, we simulate an increase of the unit cell volume of only 1% upon the whole hydration, which means that the lattice undergoes only a slight distortion. Furthermore, both the average Ow−H distance and H−Ow−H angle of the water molecules of 0.985 Å and 102.4°, respectively, and also the average Ow−Ow distance between two water molecules of 2.74 Å are in good agreement with X-ray

TABLE 4: Evolution of the Water Coordination Sphere for Each Cation as a Function of the Water Content

nH_2O/uc	Na1	Na2	Na3	Na4	Na5	Na6	Na7	Na8
1			**1**−3.056					
2	**1**−2.984		**1**−3.167					
3	**2**−2.689	**1**−2.845						
	−3.245							
4	**2**−2.652	**1**−2.625	**1**−3.104					
	−3.229							
5	**2**−2.657	**1**−2.650	**1**−3.073			**1**−3.037		
	−3.098							
6	**2**−2.631	**2**−2.424	**1**−3.026			**1**−3.027		
	−3.074	−3.002						
7	**2**−2.586	**2**−2.501	**2**−2.684			**1**−2.923		
	−3.052	−2.931	−2.733					
8	**2**−2.586	**2**−2.504	**2**−2.645	**1**−3.616		**1**−2.931		
	−3.046	−2.935	−2.648					
9	**2**−2.565	**3**-	**2**−2.651	**1**−3.702		**1**−2.982		
	−3.051	2−2.479	−2.683					
		−3.031						
		1−4.011						
10	**2**−2.606	**3**-	**2**−2.521	**2**−2.435		**1**−2.973		
	−3.048	2−2.468	−2.771	−3.965				
		−3.042						
		1−4.031						
11	**2**−2.621	**3**-	**2**−2.512	**3**−2.649		**1**−2.972		
	−3.023	2−2.408	−2.781	−3.059				
		−3.022		−3.231				
		1−4.043						
12	**2**−2.621	**3**-	**2**−2.521	**3**−2.652		**2**−3.112		
	−3.021	2−2.407	−2.754	−3.071		−3.168		
		−3.017		−3.231				
		1−4.040						
13	**2**−2.675	**3**-	**2**−2.527	**4**-		**2**−3.041		
	−2.987	2−2.439	−2.756	3−2.693		−3.495		
		−3.021		−2.718				
		1−4.093		−3.007				
				1−4.357				
14	**2**−2.676	**3**-	**2**−2.523	**4**-		**2**−3.029		**1**−3.499
	−2.994	2−2.455	−2.753	3−2.698		−3.495		
		−3.031		−2.724				
		1−4.095		−3.011				
				1−4.387				
15	**2**−2.747	**3**-	**2**−2.567	**5**-		**2**−2.963		**1**−3.619
	−3.003	2−2.454	−2.741	2−2.732		−3.444		
		−3.105		−3.203				
		1−4.025		3−4.713				
				−4.749				
				−5.143				
16	**2**−2.751	**3**-	**2**−2.591	**6**-		**2**−2.965		**1**−3.612
	−3.008	2−2.450	−2.722	2−2.812		−3.451		
		−3.100		−3.372				
		1−4.030		4−4.083				
				−4.679				
				−4.797				
				−5.288				
17	**2**−2.752	**4**-	**2**−2.602	**6**-		**2**−2.974		**1**−3.603
	−3.053	2−2.354	−2.712	2−2.815		−3.461		
		−2.953		−3.381				
		2−4.225		4−4.086				
		−4.805		−4.669				
				−4.797				
				−5.227				
18	**2**−2.753	**4**-	**2**−2.609	**7**-		**2**−2.975		**1**−3.644
	−3.087	2−2.398	−2.705	3−2.196		−3.455		
		−2.962		−2.794				
		2−4.235		−3.122				
		−4.825		4−3.995				
				−4.393				
				−4.399				
				−5.431				
19	**2**−2.752	**4**-	**2**−2.603	**8**-		**2**−2.974		**1**−3.557
	−3.046	2−2.491	−2.694	4−2.370		−3.490		
		−3.083		−3.012				
		2−4.215		−3.015				
		−4.825		−3.040				
				4−4.144				
				−4.386				
				−4.550				
				−5.629				
20	**2**−2.753	**4**-	**2**−2.615	**8**-		**2**−2.977		**2**−3.082
	−3.053	2−2.483	−2.689	4−2.391		−3.491		−3.554
		−3.076		−3.009				
		2−4.225		−3.023				
		−4.845		−3.035				
				4−4.135				
				−4.382				
				−4.573				
				−5.618				
21	**2**−2.675	**4**-	**2**−2.627	**8**-	**1**−3.121	**2**−2.998		**2**−3.005
	−3.045	2−2.446	−2.682	4−2.297		−3.498		−3.641
		−3.053		−2.927				
		2−4.146		−3.025				
		−4.765		−3.172				
				4−4.226				
				−4.533				
				−4.636				
				−5.777				
22	**2**−2.672	**4**-	**2**−2.643	**8**-	**1**−3.234	**2**−3.005	**1**−2.746	**2**−3.012
	−3.028	2−2.442	−2.686	4−2.302		−3.496		−3.632
		−3.093		−2.932				
		2−4.198		−3.024				
		−4.796		−3.181				
				4−4.221				
				−4.504				
				−4.628				
				−5.762				
23	**2**−2.663	**4**-	**2**-2.654	**8**-	**2**-	**2**−3.021	**1**−2.856	**2**−3.021
	−3.042	2−2.423	−2.682	4−2.388	1−2.836	−3.497		−3.610
		−3.012		−2.838	1−5.234			
		2−4.225		−3.043				
		−4.805		−3.202				
				4−4.272				
				−4.445				
				−4.618				
				−5.713				
24	**2**−2.661	**4**-	**2**−2.678	**9**-	**2**-	**2**−3.031	**1**−2.869	**2**−3.003
	−3.021	2−2.504	−2.723	4−2.412	1−2.830	−3.547		−3.594
		−3.059		−2.803	1−5.222			
		2−4.094		−3.112				
		−4.763		−3.196				
				5−4.332				
				−4.472				
				−4.572				
				−4.621				
				−5.734				

[a] The reported distances (Å) between Na^+ and the oxygen of the water (O_w) are classified in two distinct groups.

diffraction data reported on other hydrated zeolite systems.[6] Finally, we report in Table 4 the evolution of the water coordination sphere around the extraframework cations during the whole hydration. We observe that, in the main channels, cations 2 and 4 are surrounded by two coordination spheres corresponding to two distinct Na−Ow distance groups whereas for cations 1 and 3 only one class of Na−Ow distance is observed, corresponding to a single coordination shell. Furthermore, we observe that the maximum number of water molecules constituting the first coordination sphere is 4 and the average Na−Ow distance is about 2.8 Å. Next, the cations in the small side channels are only coordinated by water molecules located in the double 8-rings with an average Na−Ow distance of 3.2 Å, this first coordination shell being composed of a maximum number of 2 water molecules. Overall, these observations are in good qualitative agreement with data reported on hydrated Ca−mordenite.[6]

We have thus shown that the cations situated in the main channels are progressively extracted from their initial positions upon hydration of 3, 6, 7, and 11 H_2O per unit cell. They then

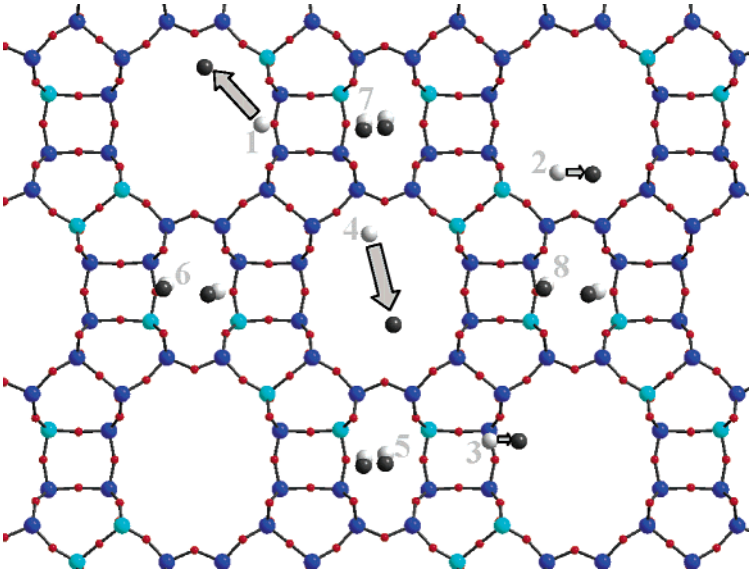

Figure 7. Representation of the extraframework cation positions in the dehydrated (light gray) and in the fully hydrated (dark gray) Na^+−mordenite. For the sake of clarity, the unit cell is extended in 2 dimensions and the water molecules are not reported.

occupy new sites that cannot be clearly identified with the crystallographic sites classified by Mortier.[6] As far as we can say, these cations are close to the water sites named Vw and VIw.[6] On the other hand, the cations in the small side channels remain trapped in the same sites I whatever the hydration level. However, their positions are slightly shifted due to the presence of water molecules in neighboring double 8-ring sites. These different types of cation motion occurring during the hydration process are summarized in Figure 7, where, for the sake of clarity, only the cation positions in the fully hydrated and dehydrated Na−mordenite structures are shown in an extended section of the mordenite structure.

We now can compare the results obtained from this simulation to those obtained experimentally by DRS. First, the population of site I remains constant whatever the H_2O content, which is well reproduced by our calculation. Second, we have observed experimentally that all the cations are trapped until 3.2 H_2O per unit cell and that beyond this hydration level, the populations of sites IV and VI dramatically decrease in the range 3.2−8.7 H_2O/uc. This range is quantitatively in good agreement with those determined (3−11 H_2O/uc) by our simulation. Finally, site I is the only one occupied in the totally hydrated structure, sites IV and VI being free of cations. This latter result is also successfully reproduced by the simulation, as we can observe in Figure 5.

Moreover, the decrease in site energies noticed experimentally when the number of water molecules increases can be interpreted microscopically by our model. In the case of the cations situated in the main channels, the water interacts directly with them and pushes them progressively away from the framework, leading to weaker and weaker cation−framework interactions as the water content increases. This is particularly well illustrated by the behavior of cation 4 during the whole hydration process. On the other hand, we have shown that cations in the small side channels are only slightly perturbed by water occupying neighboring sites. This means that the cation−water interactions over longer distances are less important than those found for the cations of the main channels. This observation would lead us to expect that the decrease in the energy of sites I is less pronounced, as has been revealed by the experiment.

Conclusion

We have adopted an atomistic simulation approach that consisted of selecting a reliable interatomic potential, to predict the locations of extraframework cations in Na−mordenite with various hydration rate. Our simulations show two different cation behaviors depending on their locations; the cations situated in the main channels are progressively extracted from their initial sites upon hydration whereas those located in the small side channels remain trapped whatever the water content. These results were in very good agreement with experimental data obtained by dielectric relaxation spectroscopy. Finally, this work allows us to provide a microscopic description of the effect of hydration on the Na−mordenites, which plays a key role in ion exchange processes in zeolites.

Acknowledgment. This research was supported through a European Communities Marie Curie Individual Fellowship: G.M. with EC Contract Number HPMF-CT-2001-01379. R.B. acknowledges the Leverhulme for funding.

References and Notes

(1) Gottardi, G.; Galli, E. *Natural Zeolites*; Springer-Verlag: Berlin, 1985; 223.
(2) Rao, C. N. R.; Natarajan, S.; Neeraj, S. *J. Am. Chem. Soc*. **2000**, *122*, 2810.
(3) Davis, P. J.; Van Bekkum, H.; Coker, E. N. *J. Chem. Educ*. **1999**, *76*, 469.
(4) Adabbo, M.; Caputo, D.; De Gennaro, B.; Pansini, M.; Collela, C. *Micropor. Mesopor. Mater*. **1999**, *28*, 315.
(5) Demontis, P.; Suffritti, G. B. *Chem. Rev.* **1997**, *97*, 2845.
(6) Mortier, W. J.; Pluth, J. J.; Smith, J. V. *Mater. Res. Bull*. **1976**, *11*, 15.
(7) Bosch, E.; Huber, S.; Weitkamp, J.; Knozinger, H. *Phys. Chem. Chem. Phys*. **1999**, *1*, 579.
(8) Meier, W. M. *Z. Kristallogr*. **1961**, *115*, 439.
(9) Pamba, M.; Maurin, G.; Devautour, S.; Vanderschueren, J.; Giuntini, J. C.; Di Renzo, F.; Hamidi, F. *Phys. Chem. Chem. Phys*. **2000**, *113* (11), 4498.
(10) Devautour, S., Vanderschueren, J.; Giuntini, J. C.; Henn, F.; Zanchetta, J. V.; Ginoux, J. L. *J. Phys. Chem. B* **1998**, *102*, 3749.
(11) Maurin, G.; Senet, P.; Devautour, S.; Gaveau, P.; Henn, F.; Van Doren, V.; Giuntini, J. C. *J. Phys. Chem. B* **2001**, *105*, 9157.
(12) Devautour, S.; Abdoulaye, A.; Giuntini, J. C.; Henn, F. *J. Phys. Chem. B* **2001**, *105*, 9297.
(13) Pissis, P.; Daoukaki-Diamanti, D. *J. Phys. Chem. Solids* **1993**, *54*, 701.

(14) Artioli, G.; Smith, J. V.; Kvick, A.; Pluth, J. J.; Stahl, K. In *Zeolites*; Dram, B., Hocevar, S., Paovnik, S., Eds.; Elsevier: Amsterdam, 1985; 249.
(15) Dyer, A.; Faghihian, F. *Micropor. Mesopor. Mater*. **1998**, *21*, 39.
(16) Ward, R. L.; McKague, L. *J. Phys. Chem. B* **1994**, *98*, 1232.
(17) Leherte, L.; Lie, G. C.; Swamy, K. N.; Clementi, E.; Derouane, E. G.; Andre, J. M. *Chem. Phys. Lett.* **1988**, *145* (3), 237.
(18) Faux, D.; Smith, W.; Forester, T. R. *J. Phys. Chem. B* **1997**, *101*, 1762.
(19) Faux, D. *J. Phys. Chem. B* **1999**, *103*, 7803.
(20) Connor, D. O.; Barnes, P.; Bates, D. R.; Lander, D. F. *Chem. Commun.* **1998**, 2527.
(21) Channon, Y. M.; Catlow, C. R. A.; Gorman, A. M.; Jackson, R. A. *Micropor. Mesopor. Mater*. **1998**, *102*, 4045.
(22) Ramirez-Cuesta, A. J.; Mitchell, P. C. H.; Parker, S.; Rodger, P. M. *Phys. Chem. Chem. Phys.* **1999**, *1*, 5711.
(23) Hill, J. R.; Minihan, A. R.; Wimmer, E.; Adams, C. J. *Phys. Chem. Phys. Chem*. **2000**, *2*, 4255.
(24) Fois, E.; Gamba, A.; Tabacchi, G.; Quartieri, S.; Vezzalini, G. *Phys. Chem. Phys. Chem*. **2001**, *3*, 4158.
(25) Almora-Barios, N.; Gomez, A.; Ruiz Salvador, A. R.; Mistry, M.; Lewis, D. W. *Chem. Commun*. **2001**, 531.
(26) Dewis, D. W.; Ruiz Salvador, A. R.; Almora Barios, N.; Gomez, A.; Mistry, M. *Mol. Simul.* **2002**, *28* (6−7), 649.
(27) Manon Higgins, F.; de Leeuw, N. H.; Parker, S. C. *J. Mater. Chem*. **2002**, *12*, 124.
(28) Maurin, G.; Senet, P.; Devautour, S.; Henn, F.; Giuntini, J. C.; Van Doren, V. E. *Comput. Mater. Sci.* **2001**, *22*, 106.
(29) Gale, J. D. *J. Chem. Soc., Faraday. Trans*. **1997**, *93*, 629.
(30) Jackson, R. A.; Catlow, C. R. A. *Mol. Simul*. **1988**, *1*, 207.
(31) Sanders, M. J.; Leslie, M.; Catlow, C. R. A. *J. Chem. Soc. Chem. Commun*. **1984**, 1271.
(32) De Leeuw, N. H.; Parker, S. C. *J. Am. Ceram*. **1999**, *82*, 3209.
(33) Allen, M. F.; Tildesley, D. *Computer Simulation of Liquids*; Oxford, Science Publication: Oxford, U.K., 1987.
(34) Coughlan, B.; Carrol, W. M.; Mc. Cann, A. *J. Chem. Soc., Faraday Trans*. **1977**, *73*, 1612.
(35) Lau, K. F.; Alper, H. E.; Thatcher, S.; Stouch, T. R. J. *Phys. Chem. B* **1994**, *98*, 8785.
(36) De Leeuw, N. H.; Parker, S. C. *Phys. Rev. B* **1998**, *58* (20), 13901.
(37) Cerius^2, Accelrys, Molecular Simulation Inc., San Diego, 1998.